

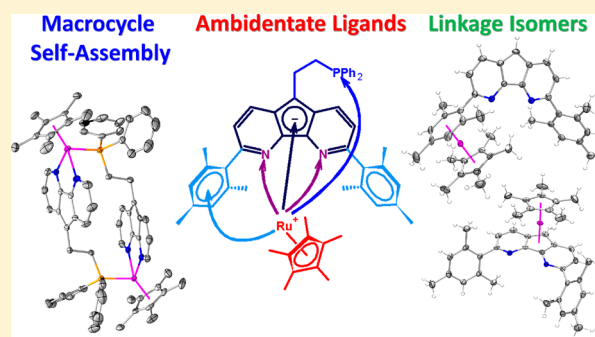
RuCp* Complexes of Ambidentate 4,5-Diazafluorene Derivatives: From Linkage Isomers to Coordination-Driven Self-Assembly

Vincent T. Annibale, Rhys Batcup, Tao Bai, Sarah J. Hughes, and Datong Song*

Davenport Chemical Research Laboratories, Department of Chemistry, University of Toronto, 80 St. George Street, Toronto, Ontario, Canada M5S 3H6.

Supporting Information

ABSTRACT: The coordination chemistry of the $\{\text{RuCp}^*\}^+$ fragment was studied toward several 4,5-diazafluorene derivatives. The ambidentate nature of these 4,5-diazafluorene derivatives with multiple coordination sites allowed for the syntheses of different linkage isomers and self-assembled macrocycles. Both a tetramer (2) and a monomer (3) of $[\text{RuCp}^*\text{L}]$ (where $\text{L}^- = 4,5\text{-diazafluorene}$) were prepared with the L^- ligand. The dimeric head-to-tail macrocycles $[\text{Cp}^*\text{Ru}(\text{L}_p\text{H})]_2\text{Cl}_2$ (4) and $[\text{Cp}^*\text{RuL}_p]_2$ (5) were obtained with the ditopic L_pH and L_p^- ligands (where $\text{L}_p\text{H} = 9\text{-}(2\text{-}(\text{diphenylphosphino})\text{ethyl})\text{-}4,5\text{-diazafluorene}$ and $\text{L}_p^- = 9\text{-}(2\text{-}(\text{diphenylphosphino})\text{ethyl})\text{-}4,5\text{-diazafluorene}$). The bulky arene-substituted $\text{L}_{\text{Mes}}\text{H}$ ligand (where $\text{L}_{\text{Mes}}\text{H} = 3,6\text{-dimesityl-}4,5\text{-diazafluorene}$) was prepared, and its coordination to $\{\text{RuCp}^*\}^+$ gave $[\text{Cp}^*\text{Ru}(\text{L}_{\text{Mes}}\text{H})]\text{Cl}$ (13). The selective syntheses of different linkage isomers of $[\text{RuCp}^*(\text{L}_{\text{Mes}})]$ (14 and 15) (where $\text{L}_{\text{Mes}}^- = 3,6\text{-dimesityl-}4,5\text{-diazafluorene}$) were also demonstrated.



INTRODUCTION

Ambidentate ligands, which feature several potential coordination sites, provide an opportunity to form linkage isomers or potentially serve as building blocks for coordination-driven self-assembly.^{1–6} Organometallic Ru fragments have been used in the self-assembly of a variety of supramolecular complexes and macrocycles, where several display intriguing photophysical, molecular recognition, and anticancer properties.^{6–12}

Our group has been actively exploring the chemistry and reactivity of the 4,5-diazafluorene (LH) and 4,5-diazafluorene ligands (L^-) (Chart 1).^{13–18} Diazafluorene is a bipyridyl ligand

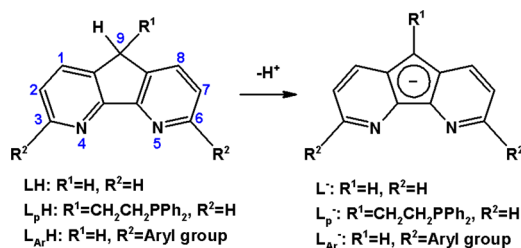
exception where both coordination sites of the ligand are used in $[\text{Pd}(\text{L})(\text{PPh}_3)\text{Cl}]_2$,¹³ where L^- was bound to Pd(II) through both one of the N-donors and the anionic C-donor of the ligand backbone in an $\eta^1(\sigma)$ -fashion.

Recently we have demonstrated that in the heterodinuclear complex $[(\text{IPr})\text{Cu}(\text{L})\text{Pt}(\text{Ph})_2]$ the Cu(I) center is bound to the carbon site of diazafluorene in an $\eta^1(\pi)$ -fashion and the Pt(II) center is coordinated to the N,N-chelate site.¹⁹

We later installed a phosphine arm at the 9-position of diazafluorene to give the L_pH ligand, which can also be deprotonated to form the L_p^- ligand (Chart 1).¹⁸ We demonstrated ligand transfer of L_p^- from Cu(I) to either Rh(I) or Au(I), resulting in macrocyclic complexes.¹⁸ L_pH and L_p^- are also ambidentate ligands with phosphine and N-donor coordination sites. In addition, L_p^- can also anchor a metal in the P,C-coordination site. Recently we have demonstrated that in the heterodinuclear complex $[(\text{IPr})\text{Cu}(\text{L}_p)\text{Pt}(\text{Ph})_2]$ the tethered phosphine of L_p^- helps anchor the Pt(II) center onto the carbon site of the diazafluorene, and the Cu(I) center is bound to the N,N-chelate site.¹⁹

The installation of aryl groups *ortho* to the N-donors of the diazafluorene framework can provide steric protection and allow access to reactive low-coordinate N-bound metal centers ($\text{L}_{\text{Ar}}\text{H}$ and L_{Ar}^- ; see Chart 1). As a monoanionic α -diimine ligand, L_{Ar}^- is analogous to the β -diketiminato ligand (also known as *nacnac*),²⁰ e.g., overall -1 charge, N-donor set, and

Chart 1. Ambidentate Ligands Used in This Study



with a methylene linker that can be deprotonated to form the monoanionic diazafluorene ligand. An interesting feature of the ambidentate L^- ligand is that it potentially has two metal-binding sites: the N-donors and the C-donors of the central Cp*-like ring. However in most examples L^- binds metals with its nitrogen donors, without utilizing the C-donors. One

Received: August 22, 2013

Published: October 8, 2013



noninnocent carbon backbone.^{17,21–27} These bulkier diazafluorene derivatives are also ambidentate: L_{Ar}^- has a N,N-chelate site and the C-donors of the central Cp^- moiety; in addition, there is also the possibility of the aryl substituent participating in bonding. Similar to 4,5-diazafluorene derivatives, ambidentate bis-imine-functionalized pentafulvenes also have a Cp^- moiety and a κ^2 -[N,N] chelate.^{28–30}

The Cp^* ($C_5Me_5^-$) ligand has been used extensively in organometallic chemistry as a sterically demanding, electron-donating ligand to stabilize reactive or coordinatively unsaturated complexes.^{31–39} Tilley^{40–45} and Caulton^{46–50} have demonstrated the use of the $\{RuCp^*\}^+$ fragment in reactive, π -stabilized unsaturated species including two-legged piano-stool complexes. Stradiotto and co-workers have also examined the chemistry of coordinatively unsaturated zwitterionic $RuCp^*$ complexes and cases of linkage isomerism and small-molecule activation.^{51–57} Structurally the Cp^* ligand also blocks three *fac*-coordination sites of Ru(II),⁷ allowing for the self-assembly of molecular architectures with $RuCp^*$ half-sandwich vertices. Here we report the syntheses of $RuCp^*$ complexes of 4,5-diazafluorene derivatives. The ambidentate, multifunctional ligands utilized enabled the isolation of linkage isomers and self-assembled macrocycles. We also present the syntheses of diazafluorene ligands with aryl substituents *ortho* to the N-donors.

EXPERIMENTAL SECTION

General Information. All air- or moisture-sensitive operations were performed using Schlenk/vacuum-line techniques under dinitrogen or in a dinitrogen atmosphere glovebox from MBraun. Workups for organic reactions were done in air. High-temperature and -pressure reactions were done in stainless steel Parr acid digestion vessels and heated with a Parr 5000 multireactor heater-stirrer system. 4,5-Diazafluorene (LH),^{58,59} L_pH ,¹⁸ and $[RuCp^*(\mu^3-Cl)]_4$ ⁶⁰ were synthesized from literature procedures. Compound 6 was synthesized by a modified literature procedure using toluene as the solvent.^{61,62} Compound 7 was synthesized using a literature procedure from Guo and co-workers,⁶² with the following modifications to the workup. After the reaction the $HOtBu$ solvent was removed by rotary evaporation, the crude was extracted with $CHCl_3$, and the organic layer was washed with H_2O . To the $CHCl_3$ extract was added 5% by volume of methanol along with $MgSO_4$, and the mixture was filtered through a silica gel plug. Removal of the solvent yields 1H NMR pure compound 7 in 83% yield. Compounds 8^{61,62} and 9⁶¹ were synthesized directly from literature procedures. Thin-layer chromatography was performed with silica gel 60 F₂₅₄ Al-backed TLC plates, spots were visualized under UV, and column chromatography was performed using SiliaFlash P60 silica gel from Silicycle. Glassware was dried overnight in a 180 °C oven prior to use except for NMR tubes, which were dried overnight in a 60 °C oven. THF, toluene, DME, pentane, hexanes, diethyl ether, benzene, and benzene-*d*₆ were dried over Na/benzophenone and either distilled under nitrogen or vacuum-transferred before use. DMSO-*d*₆ was dried over CaH_2 at 80 °C overnight and vacuum distilled prior to use. CD_2Cl_2 and $CDCl_3$ were dried over CaH_2 and vacuum transferred prior to use. 1H , ^{31}P , and ^{13}C NMR spectra were recorded on a Varian 300 MHz, Varian 400 MHz, Bruker Avance III 400 MHz, or Agilent DD2-600 MHz NMR spectrometer. All chemical shifts are reported in ppm relative to residual protio-solvent peaks, and ^{31}P NMR are referenced externally using 85% H_3PO_4 in a flame-sealed capillary. GC-MS analyses were carried out on an Agilent 7980A GC system (equipped with an HP-5 column) connected with a 5975C inert XL MSD using hydrogen as the carrier gas. Elemental analyses were performed by ANALEST at the University of Toronto.

Synthesis of $[RuCp^*(LH)Cl]$ (1). In the glovebox 230 mg (0.21 mmol) of $[RuCp^*(\mu^3-Cl)]_4$ was dissolved in 7 mL of THF, and 150 mg (0.89 mmol) of LH was added, resulting in a dark purple

precipitate. After 2 h with no agitation the dark purple microcrystalline precipitate of 1 was collected by filtration and washed with a minimal amount of THF and hexanes (295 mg, 75% yield). Crystals of X-ray diffraction quality were grown from vapor diffusion of hexanes into a THF solution of 1. 1H NMR (600 MHz, CD_2Cl_2 , δ): 8.93 (d, $J = 5.3$ Hz, 2H), 7.80 (d, $J = 7.5$ Hz, 2H), 7.45 (dd, $J = 7.6, 5.2$ Hz, 2H), 4.13 (s, 2H), 1.74 (s, 15H). ^{13}C NMR (151 MHz, CD_2Cl_2 , δ): 162.23, 148.89, 135.45, 131.60, 125.40, 75.61, 36.71, 10.37. 1H NMR (600 MHz, $CDCl_3$, δ): 8.89 (d, $J = 5.2$ Hz, 2H), 7.72 (d, $J = 7.5$ Hz, 2H), 7.37 (dd, $J = 7.5, 5.3$ Hz, 2H), 4.05 (s, 1H), 4.04 (s, 1H), 1.71 (s, 15H). ^{13}C NMR (151 MHz, $CDCl_3$, δ): 162.14, 148.73, 134.83, 131.18, 124.86, 75.18, 36.41, 10.43. Anal. Calcd for $C_{21}H_{23}N_2RuCl$: C, 57.33; H, 5.27; N, 6.37. Found: C, 57.25; H, 5.21; N, 6.28.

Synthesis of $[Ru(Cp^*)(L)]_4$ (2). Method A. In the glovebox, 15 mg (89.12 μ mol) of LH and 10 mg (89.12 μ mol) of $KOtBu$ were dissolved in 3 mL of THF and stirred for 2 h, resulting in a purple solution of KL. Addition of the KL solution to 24.2 mg (22.30 μ mol) of $[RuCp^*(\mu^3-Cl)]_4$ dissolved in 8 mL of THF yielded purple X-ray diffraction quality crystals of 2 after 5 days. The supernatant containing KCl and other impurities was decanted from the crystals, and the crystals were washed with 5 mL of THF and dried under vacuum (11 mg, 31% yield).

Method B. In the glovebox, 115 mg (0.26 mmol) of 1 was partially dissolved in 5 mL of THF, and 520 μ L of 0.5 M $K[HB(Et)_3]$ in THF was added, giving a dark red-brown solution and H_2 evolution. The reaction mixture was stirred at RT for 1 h; then the solvent was removed under vacuum, and the residue was extracted into benzene, filtered, and left to stand. After 3 days dark purple, large, X-ray diffraction quality crystals of 2·2(C_6H_6) had formed. The supernatant was pipetted off, and the crystals were washed with pentane and dried under vacuum (24 mg, 22% yield based on 2·(C_6H_6)). The poor solubility of complex 2 in all common NMR solvents hindered solution-based NMR characterization. Anal. Calcd for $(C_{84}H_{88}N_8Ru_4)(C_6H_6)_2$: C, 63.89; H, 5.60; N, 6.62. Found: C, 63.52; H, 5.48; N, 6.44.

Synthesis of $[RuCp^*(L)]$ (3). In the glovebox, 67 mg (0.398 mmol) of LH was dissolved in 4 mL of THF and added dropwise to a stirring suspension of 35 mg (1.46 mmol) of pentane-washed NaH suspended in 4 mL of THF. Upon the addition of LH, H_2 evolution was observed, and the reaction mixture was stirred at RT for 30 min, giving a purple-pink solution along with excess NaH. The NaL solution was simultaneously filtered and added dropwise to a stirred solution-suspension of 98 mg (0.09 mmol) of $[RuCp^*(\mu^3-Cl)]_4$ in 6 mL of THF over the course of 15 min. After the addition of NaL is complete the solution-suspension appeared brown, and the reaction mixture was stirred at RT for 2 h. The solvent and volatiles were removed under vacuum, and the brown residue was extracted into toluene and filtered to remove a dark precipitate and KCl. The solvent from the orange filtrate was removed under vacuum, and the product was triturated with pentane (63 mg, 43% yield). X-ray diffraction quality crystals of 3 were grown by vapor diffusion of hexanes into a benzene solution. 1H NMR (600 MHz, $CDCl_3$, δ): 8.71 (dd, $J = 3.8, 1.6$ Hz, 2H), 7.66 (dd, $J = 8.7, 1.6$ Hz, 2H), 6.86 (dd, $J = 8.7, 3.8$ Hz, 2H), 5.12 (s, 1H), 1.31 (s, 15H). ^{13}C NMR (151 MHz, $CDCl_3$, δ): 149.17, 135.18, 117.74, 107.07, 89.27, 81.21, 56.80, 9.47. 1H NMR (600 MHz, C_6D_6 , δ): 8.74–8.61 (m, 2H), 7.21 (dd, $J = 8.7, 1.5$ Hz, 2H), 6.41 (dd, $J = 8.7, 3.8$ Hz, 2H), 4.81 (s, 1H), 1.25 (s, 15H). ^{13}C NMR (151 MHz, C_6D_6 , δ): 149.18, 134.59, 117.79, 107.88, 89.53, 81.02, 56.92, 9.46. Anal. Calcd for $C_{21}H_{22}N_2Ru$: C, 62.51; H, 5.50; N, 6.94. Found: C, 62.86; H, 5.66; N, 7.11.

Synthesis of $[RuCp^*(L_pH)]_2Cl_2$ (4). In the glovebox, 10 mg (9.2 μ mol) of $[RuCp^*(\mu^3-Cl)]_4$ was dissolved in 12 mL of THF, and 14 mg (36.8 μ mol) of L_pH was dissolved in 8 mL of THF. The L_pH solution was carefully layered on top of the $[RuCp^*(\mu^3-Cl)]_4$ solution, resulting in a purple solution. Slow evaporation of the THF solvent yielded orange crystals of 4 suitable for X-ray crystallographic analysis. After 8 days, the supernatant was decanted; the crystals were washed with cold THF and dried under vacuum (10.8 mg, 45% yield). 1H NMR (DMSO-*d*₆, 400 MHz, δ): 8.75 (d, $^3J = 5.47$ Hz, 2H), 7.70–7.59 (m, 10H), 7.50 (dd, $^3J = 7.55$ Hz, $^3J = 5.44$ Hz, 2H), 7.40 (d, $^3J = 7.59$ Hz, 2H), 4.16 (t, $^3J = 7.40$ Hz, 1H), 1.86–1.80 (m, 2H), 1.11 (d, $^4J_{H-P}$

= 1.23 Hz, 15H), 0.18–0.14 (m, 2H). $^{13}\text{C}\{^1\text{H}\}$ NMR (DMSO- d_6 , 100 MHz, δ): 160.2, 151.8, 137.9, 133.4, 133.1, 132.7 (d, $J_{\text{C-P}} = 11.8$ Hz), 132.5, 130.3, 128.8 (d, $J_{\text{C-P}} = 9.6$ Hz), 126.6, 84.0 (d, $J_{\text{C-P}} = 1.8$ Hz), 8.6. $^{31}\text{P}\{^1\text{H}\}$ NMR (DMSO- d_6 , 162 MHz, δ): 37.7. Anal. Calcd for $\text{C}_{70}\text{H}_{72}\text{N}_4\text{P}_2\text{Ru}_2\text{Cl}_2$: C, 64.46; H, 5.56; N, 4.30. Found: C, 64.07; H, 5.72; N, 4.06.

Synthesis of $[\text{RuCp}^*(\text{L}_p)_2]$ (5). *Method A.* In the glovebox, 50 mg (131.4 μmol) of L_pH and 14.7 mg (131.4 μmol) of KOtBu were dissolved in 2 mL of THF and stirred for 2 h, resulting in a purple solution of KL_p . To the solution of KL_p was added 35.7 mg (32.9 μmol) of solid $[\text{RuCp}^*(\mu^3\text{-Cl})_4]$, and the mixture was stirred for 2 h. The solvent was removed under vacuum, leaving a brown residue, which was extracted into 10 mL of toluene and filtered. The brown toluene solution was heated at 100 °C overnight, resulting in a bright green solution. The green solution was filtered, and the solvent was removed under vacuum to give complex 5 (60 mg, 74% yield). X-ray diffraction quality crystals can be grown by either vapor diffusion of hexanes into a benzene solution (5) or vapor diffusion of pentane into a DME solution (5·pentane).

Method B. To 18.6 mg (14.25 μmol) of 4 was added 1 mL of a 29.7 $\mu\text{mol/mL}$ solution of KOtBu, and the mixture was left to sit overnight at RT to yield a green solution. The solvent and volatiles were removed under vacuum, and the residue was extracted into toluene, filtered, and dried under vacuum to give complex 5 (16.2 mg, 92% yield). ^1H NMR (C_6D_6 , 300 MHz): δ 7.85 (d, $^3J = 4.72$ Hz, 2H), 7.71–7.65 (m, 4H), 7.35–7.26 (m, 6H), 7.23 (dd, $^3J = 7.22$ Hz, $^4J = 1.39$ Hz, 2H), 6.95 (dd, $^3J = 7.76$ Hz, $^3J = 4.71$ Hz, 2H), 2.54–2.44 (m, 2H), 1.37 (d, $^4J_{\text{H-P}} = 1.37$ Hz, 15H), –0.55 to –0.66 (m, 2H). $^{13}\text{C}\{^1\text{H}\}$ NMR (C_6D_6 , 100 MHz): δ 142.5, 135.2, 134.9, 134.6, 133.5 (d, $J_{\text{C-P}} = 10.59$ Hz), 129.1 (d, $J_{\text{C-P}} = 1.74$), 126.5, 124.3, 121.8, 116.8, 95.1 (d, $J_{\text{C-P}} = 9.89$ Hz), 82.4 (d, $J_{\text{C-P}} = 2.18$ Hz), 9.9. $^{31}\text{P}\{^1\text{H}\}$ NMR (C_6D_6 , 121.5 MHz): δ 38.0. Anal. Calcd for $\text{C}_{70}\text{H}_{70}\text{N}_4\text{P}_2\text{Ru}_2$ ($\text{C}_4\text{H}_{10}\text{O}_2$): C, 67.25; H, 6.10; N, 4.24. Found: C, 66.79; H, 5.90; N, 4.31.

Synthesis of 3,6-Dichloro-4,5-diazafluoren-9-one (10). In air 4.533 g (16.2 mmol) of freshly powdered yellow 2,9-dichloro-1,10-phenanthroline-5,6-dione (9) and 2.164 g (38.6 mmol) of KOH were dissolved/suspended in 220 mL of H_2O and heated to reflux with vigorous stirring. After 10 min of reflux a dark brown reaction mixture resulted. An aqueous solution consisting of 1.951 g (12.3 mmol) of KMnO_4 dissolved in 220 mL of H_2O was heated to 60 °C, and the warm KMnO_4 solution was added dropwise to the vigorously stirred, refluxing, brown reaction mixture over the course of 3.5 h. After the addition of the KMnO_4 solution was complete the dark reaction mixture was left to reflux overnight. The reaction mixture was cooled to RT and extracted with 3 \times 300 mL of DCM, the combined DCM extracts were dried over MgSO_4 and filtered, and the solvent was removed by rotary evaporation. The crude product was purified by silica gel column chromatography eluting initially with DCM, gradually increasing the amount of EtOAc in the elution solvent until a final elution solvent of DCM–EtOAc (10:1). After chromatography the solvent was removed by rotary evaporation, and the product was dried under high vacuum to give 10 as a pale yellow microcrystalline solid (2.558 g, 63% yield). X-ray diffraction quality crystals were obtained by vapor diffusion of pentane into a CHCl_3 solution of 10. $R_f = 0.48$ (DCM). ^1H NMR (400 MHz, CDCl_3 , δ): 7.95 (d, $J = 7.9$ Hz, 2H), 7.43 (d, $J = 7.9$ Hz, 2H). ^{13}C NMR (101 MHz, CDCl_3 , δ): δ 187.02, 163.11, 158.42, 133.85, 128.20, 126.07.

Synthesis of 3,6-Dimesityl-4,5-diazafluoren-9-one (11). In a Schlenk flask under a dinitrogen atmosphere 1.990 g (7.9 mmol) of 10 and 3.884 g (23.68 mmol) of 2,4,6-trimethylphenylboronic acid were dissolved in 200 mL of toluene, and 100 mL of 1.7 M Na_2CO_3 was added. The mixture was thoroughly degassed; then 778 mg (0.67 mmol) of $\text{Pd}(\text{PPh}_3)_4$ was quickly added. The yellow biphasic reaction mixture was vigorously stirred and heated in a 115 °C oil bath overnight. After the reaction mixture cooled to RT the toluene and aqueous phases were separated, and the aqueous phase was extracted with 3 \times 100 mL of DCM. The combined organic extracts were dried over MgSO_4 and filtered, and the solvent was removed by rotary evaporation. The crude product was purified by silica gel column

chromatography first eluting with hexanes and gradually increasing the amount of EtOAc until a final elution solvent of hexanes–EtOAc (8:1). After chromatography the solvent was removed by rotary evaporation, followed by drying the product under high vacuum, giving 11 as a bright yellow solid with yellow luminescence under 365 nm irradiation (3.137 g, 95% yield). $R_f = 0.73$ (hexanes–EtOAc, 2:1). ^1H NMR (400 MHz, CDCl_3 , δ): 8.06 (d, $J = 7.7$ Hz, 2H), 7.26 (d, $J = 7.6$ Hz, 2H), 6.89 (s, 4H), 2.30 (s, 6H), 2.07 (s, 12H). ^{13}C NMR (100 MHz, CDCl_3 , δ): 189.85, 166.90, 164.05, 137.99, 137.19, 135.61, 131.57, 128.30, 128.01, 125.97, 21.23, 20.41.

Synthesis of 3,6-Dimesityl-4,5-diazafluorene ($\text{L}_{\text{Mes}}\text{H}$) and 9,9'-Bi-3,6-dimesityl-4,5-diazafluorenyl (12). In parallel, two Parr acid digestion vessels were each charged with 570 mg (total of 1.140 g, 2.72 mmol) of 11 and 12 mL of hydrazine hydrate, sealed, and heated for 7.5 h at 180 °C. After cooling to RT overnight the reaction mixtures from the two bombs were combined and extracted with 3 \times 25 mL of DCM. The DCM extracts were dried over MgSO_4 and filtered, and the solvent was removed by rotary evaporation. The TLC plate revealed two main products, which both fluoresce bright blue under 364 nm irradiation: $\text{L}_{\text{Mes}}\text{H}$ with $R_f = 0.5$ and 12 with $R_f = 0.2$ (hexanes–EtOAc, 3:1). Silica gel column chromatography was performed eluting with hexanes, initially gradually increasing the amount of EtOAc until a final hexanes–EtOAc (3:1) until all of the 3,6-dimesityl-4,5-diazafluorene had eluted off the column. The solvent was removed by rotary evaporation, and the product was dried under high vacuum to give 836 mg (75% yield) of $\text{L}_{\text{Mes}}\text{H}$ as a white solid. X-ray diffraction quality crystals were grown by diffusion of hexanes into a toluene solution of 3,6-dimesityl-4,5-diazafluorene and placing the mixture in a –30 °C freezer. The silica gel column was flushed with EtOAc–MeOH (100:1) elution solvent until all of the 12 had eluted off the column. The solvent was removed by rotary evaporation, and the product was dried under high vacuum to give 130 mg (12% yield) of 12 as a white solid. X-ray diffraction quality crystals were grown by vapor diffusion of diethyl ether into a chloroform solution of 12.

Characterization of $\text{L}_{\text{Mes}}\text{H}$. ^1H NMR (400 MHz, CDCl_3 , δ): 7.95 (d, $J = 7.8$ Hz, 2H), 7.22 (d, $J = 7.8$ Hz, 2H), 6.89 (s, 4H), 3.95 (s, 2H), 2.30 (s, 6H), 2.05 (s, 12H). ^{13}C NMR (101 MHz, CDCl_3 , δ): 160.14, 159.35, 138.23, 137.08, 136.04, 135.66, 132.96, 127.97, 123.74, 32.07, 21.19, 20.48. Anal. Calcd for $\text{C}_{29}\text{H}_{28}\text{N}_2$: C, 86.10; H, 6.98; N, 6.92. Found: C, 85.92; H, 6.97; N, 6.95.

Characterization of 12. ^1H NMR (500 MHz, CD_2Cl_2 , δ): 7.48 (br s, 4H), 7.06 (br d, $J = 8.0$ Hz, 4H), 6.89 (s, 8H), 5.11 (s, 2H), 2.29 (s, 12H), 1.96 (br s, 24H). ^{13}C NMR (126 MHz, CDCl_3 , δ): 161.08, 159.25, 137.68, 137.18, 136.59, 135.63, 131.93, 127.89, 123.57, 44.85, 21.06, 20.22. Anal. Calcd for $\text{C}_{58}\text{H}_{54}\text{N}_4 \cdot 0.27(\text{CHCl}_3) \cdot 0.49(\text{O}(\text{C}_2\text{H}_5)_2)$ (ratio of 12 to CHCl_3 and Et_2O determined by integration of ^1H NMR spectrum): C, 82.62; H, 6.79; N, 6.39. Found: C, 83.16; H, 6.94; N, 6.43.

Selective Synthesis of 3,6-Dimesityl-4,5-diazafluorene ($\text{L}_{\text{Mes}}\text{H}$). $\text{L}_{\text{Mes}}\text{H}$ can be synthesized more selectively (without formation of the 12 byproduct) and with a higher yield using a procedure analogous to that above. The only differences in procedures were the quantity of 11 per reaction bomb and the reaction time. In parallel, 10 Parr acid digestion vessels were each charged with 360 mg (total of 3.6 g, 8.6 mmol) of 11 and 12 mL of hydrazine hydrate, sealed, and heated at 180 °C for 24 h. Workup was performed similar to what was mentioned above (3.198 g, 92% yield).

Synthesis of $[\text{RuCp}^*(\text{L}_{\text{Mes}}\text{H})]\text{Cl}$ (13). In the glovebox, 145 mg (0.13 mmol) of $[\text{RuCp}^*(\mu^3\text{-Cl})_4]$ and 214 mg (0.52 mmol) of $\text{L}_{\text{Mes}}\text{H}$ were dissolved in 15 mL of THF and left to sit at RT for 7 days (no stirring). After 7 days colorless X-ray diffraction quality crystals of 13·(THF) had formed, and the crystals were collected by filtration, washed with THF and hexanes, and dried under vacuum (242 mg, 67% yield). ^1H NMR (600 MHz, DMSO- d_6 , δ): 8.23 (d, $J = 7.8$ Hz, 1H), 8.19 (d, $J = 7.8$ Hz, 1H), 7.56 (d, $J = 7.8$ Hz, 1H), 7.37 (d, $J = 7.8$ Hz, 1H), 6.95 (s, 2H), 5.89 (s, 2H), 4.14 (s, 2H), 2.28 (s, 3H), 2.16 (s, 3H), 2.04 (s, 6H), 1.89 (s, 6H), 1.87 (s, 15H). ^{13}C NMR (151 MHz, DMSO- d_6 , δ): 158.62, 158.49, 157.65, 151.73, 138.08, 137.79, 136.58, 136.42, 135.04, 134.18, 133.75, 128.03, 124.30, 124.14, 105.31, 99.79, 98.38, 94.88, 88.55, 31.86, 20.66, 20.00, 17.28, 16.91, 9.46. Anal. Calcd

for $(C_{39}H_{43}N_2RuCl) \cdot 1.5(OC_4H_8)$ (ratio of complex **13** to THF determined by integration of 1H NMR spectrum): C, 68.90; H, 7.07; N, 3.57. Found: C, 68.43; H, 7.14; N, 3.69.

Synthesis of Arene Isomer $[RuCp^*(L_{Mes})]$ (14**).** In the glovebox, 98 mg (0.14 mmol) of **13** was suspended in 10 mL of THF, and 16 mg (0.14 mmol) of $KOtBu$ dissolved in 10 mL of THF was added, yielding a red solution, which was stirred at RT overnight. After overnight the red reaction mixture was filtered, and toluene was layered carefully on top, yielding red X-ray diffraction quality crystals, which were collected by filtration and dried under vacuum (55 mg, 59% yield). 1H NMR (600 MHz, $DMSO-d_6$, δ): 7.75 (d, $J = 8.3$ Hz, 1H), 7.71 (d, $J = 8.4$ Hz, 1H), 6.88 (s, 2H), 6.87 (d, $J = 8.4$ Hz, 1H), 6.82 (d, $J = 8.3$ Hz, 1H), 5.93 (s, 1H), 5.75 (s, 2H), 2.27 (s, 3H), 2.13 (s, 3H), 2.12 (s, 6H), 1.98 (s, 6H), 1.92 (s, 15H). ^{13}C NMR (151 MHz, $DMSO-d_6$, δ): 138.12, 135.82, 134.32, 132.46, 127.80, 127.50, 122.06, 117.63, 116.21, 108.92, 98.95, 94.17, 88.73, 78.40, 20.68, 20.67, 17.60, 17.36, 9.62. Anal. Calcd for $(C_{39}H_{42}N_2Ru) \cdot (C_7H_8) \cdot 0.5(OC_4H_8)$ (ratio of **14** to toluene and THF solvents determined from integration of 1H NMR spectrum of EA sample): C, 75.06; H, 7.09; N, 3.65. Found: C, 74.76; H, 6.67; N, 3.41.

Synthesis of Sandwich Isomer $[RuCp^*(L_{Mes})]$ (15**).** In the glovebox, 214 mg (0.53 mmol) of $L_{Mes}H$ and 66 mg (0.59 mmol) of $KOtBu$ were dissolved in 3 mL of THF, giving a deep red solution of KL_{Mes} , which was left at RT for 30 min. The solution of KL_{Mes} was then added to 143 mg (0.13 mmol) of $[RuCp^*(\mu^3-Cl)]_4$ dissolved in 4 mL of THF, resulting in an orange solution of **15**. After 1 h the volatiles were removed under vacuum, the orange residue was extracted into toluene and filtered, and the solvent was removed under vacuum, giving an orange microcrystalline sample of **15** (300 mg, 88% yield). X-ray diffraction quality crystals can be grown by either vapor diffusion of Et_2O into a THF solution ($15 \cdot Et_2O$) or vapor diffusion of hexanes into a benzene solution ($15 \cdot C_6H_6$). 1H NMR (600 MHz, $CDCl_3$, δ): 7.73 (d, $J = 8.8$ Hz, 2H), 6.90 (d, $J = 8.8$ Hz, 2H), 6.88 (s, 4H), 5.12 (s, 1H), 2.30 (s, 6H), 2.18 (br s, 12H), 1.59 (s, 15H). ^{13}C NMR (151 MHz, $CDCl_3$, δ): 159.79, 138.92, 136.95, 134.96, 129.18, 128.37, 121.00, 108.27, 87.18, 82.34, 56.88, 21.22, 20.97, 11.03. Anal. Calcd for $(C_{39}H_{42}N_2Ru) \cdot 0.6(C_7H_8)$ (ratio of **15** to toluene determined from integration of 1H NMR spectrum of EA sample): C, 74.64; H, 6.79; N, 4.03. Found: C, 74.98; H, 7.03; N, 3.88.

X-ray Crystallography. The X-ray diffraction data were collected on a Bruker Kappa Apex II diffractometer and processed with the Bruker Apex 2 software package.⁶³ Data were collected with graphite-monochromated Mo $K\alpha$ radiation ($\lambda = 0.71073$ Å) at 150 K controlled by an Oxford Cryostream 700 series low-temperature system. The structures were solved by the direct methods or Patterson method and refined using SHELX-2013.⁶⁴ The residual electron density from disordered solvent molecules in the lattices of **2**, **4**, **5** (pentane), and **13**·(THF) was removed with the SQUEEZE function of PLATON,⁶⁵ and their contributions were excluded in the formula. The disordered Cp^* ligand in complex **1** was modeled over three positions. Non-hydrogen atoms were refined anisotropically except for disordered portions, and hydrogen atoms were calculated using the riding model. The selected crystallographic data are summarized in Table S1.

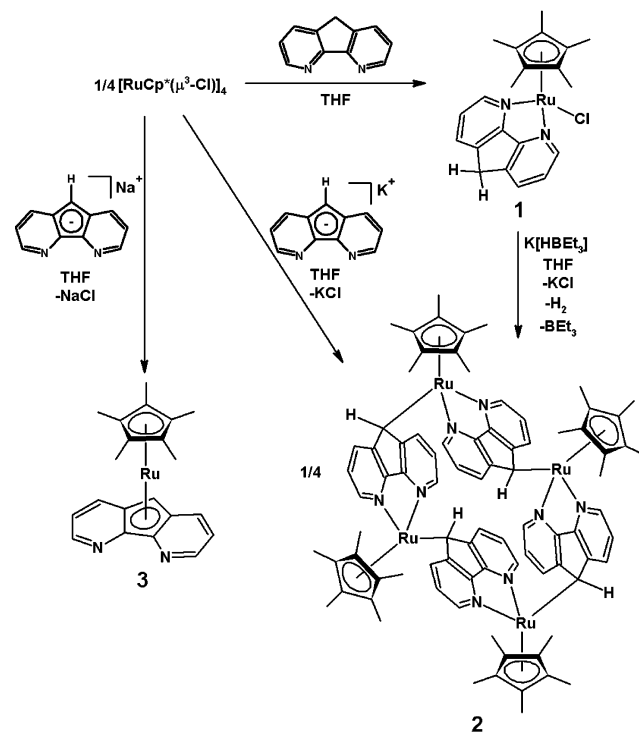
DFT Calculations. All calculations were performed using the Gaussian 09 software package⁶⁶ and B3LYP^{67,68} method. Ruthenium was treated with the SDD basis set with an effective core potential, while other elements were treated with the 6-31G* basis set. The geometry optimizations were performed with no symmetry constraint. Vibrational frequency analyses were performed on all optimized structures to obtain thermodynamic data.

RESULTS AND DISCUSSION

Coordination Chemistry of LH and L^- . We initially explored the coordination chemistry of LH and ambidentate L^- . The half-sandwich complex $[RuCp^*(\mu^3-Cl)]_4$ first reported by Fagan and co-workers proved to be a highly versatile $RuCp^*$ synthon.⁶⁰ The addition of LH to 0.25 equiv of $[RuCp^*(\mu^3-Cl)]_4$ resulted in the precipitation of deep purple microcrystal-

line complex **1** (Scheme 1). Complex **1** is soluble in DCM or chloroform, slightly soluble in THF, DME, benzene, and

Scheme 1. Syntheses of Complexes **1**, **2**, and **3**



toluene, and insoluble in diethyl ether, pentane, and hexanes. When complex **1** was dissolved in $DMSO-d_6$, the deep purple solution formed initially turned bright orange within a few seconds; the 1H NMR spectrum showed signals of free LH and a singlet belonging to Cp^* , likely indicating ligand substitution with $DMSO-d_6$ had occurred. Compound **1** is air-sensitive in solution. When a $CDCl_3$ solution of **1** was exposed to air, uncoordinated 4,5-diazafluoren-9-one was observed by 1H NMR. Previously we had reported the selective oxidation of the CH_2 moiety of the LH ligand by air in the complex $[RuCl_2(LH)(PPh_3)_2]$, giving a Ru-diazafluorenone complex.¹⁵ Free LH with typically unreactive $C(sp^3)-H$ bonds is air-stable, but coordinated LH in complex **1** reacts with O_2 in air. The 1H NMR spectrum of complex **1** in dry and deoxygenated $CDCl_3$ revealed two singlets at 4.05 and 4.04 ppm belonging to the two inequivalent methylene protons of the coordinated LH ligand. The 1H NMR in CD_2Cl_2 revealed a singlet at 4.13 ppm belonging to the methylene group of the coordinated LH ligand. Crystals of complex **1** were obtained by vapor diffusion of hexanes into a THF solution (Figure 1). Complex **1** crystallized in the monoclinic space group $C2/c$, where the *cis*-N donors of LH and the chloride are coordinated to the $RuCp^*$ half-sandwich. The bite angle of LH, $N1-Ru1-N2$, is $79.3(1)^\circ$.

It was thought that compound **1** might serve as an entry point to bifunctional small-molecule activation and catalysis. Upon deprotonation of coordinated LH in complex **1**, a coordinatively unsaturated " $RuCp^*(L^-)$ " hypothetically may engage in long-range metal-ligand cooperative activation of small molecules.^{69–73} Previously we showed that a metal-dinitrogen complex $[Ru(L)(PPh_3)_2(H)(N_2)]$ forms upon deprotonation of coordinated LH, and $[Ru(L)(PPh_3)_2(H)(N_2)]$ reversibly splits H_2 between the Ru(II) center and L^- .¹⁶

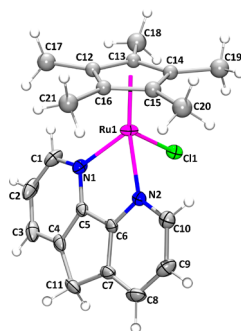


Figure 1. X-ray crystal structure of **1**. Non-hydrogen atoms are shown as 30% probability ellipsoids, and H atoms are shown as spheres of arbitrary radius. Only one orientation of the disordered Cp* ligand is shown for clarity. Selected distances (Å) and angles (deg): Ru1–N1, 2.185(3); Ru1–N2, 2.197(3); Ru1–Cl1, 2.4683(9); Ru1–cent(C12–C16), 1.7492(3); N1–Ru1–N2, 79.3(1); N1–Ru1–Cl1, 81.84(8); N2–Ru1–Cl1, 87.94(8).

The addition of 1 equiv of $\text{K}[\text{HBEt}_3]$ to complex **1** followed by extraction into benzene yielded dark purple X-ray quality crystals of $2 \cdot 2(\text{C}_6\text{H}_6)$ after 3 days (Scheme 1). The benzene extraction must be carried out soon after the reaction with $\text{K}[\text{HBEt}_3]$ in order to obtain analytically pure crystals of $2 \cdot 2(\text{C}_6\text{H}_6)$ free of KCl and other impurities. Complex **2** is insoluble in all common organic solvents after it has crystallized, and thus solution-based NMR spectroscopy was not possible. Compound $2 \cdot 2(\text{C}_6\text{H}_6)$ crystallizes in the triclinic space group $\bar{P}1$, with a crystallographically imposed inversion center in the middle of the cavity formed by the tetramer. Coordination-driven self-assembly of the tetraruthenamacrocycle **2** occurs as a result of the ambidentate nature of the L^- ligand. The four L^- ligands all engage in both κ^2 -[N,N] and $\eta^1(\sigma)$ coordination modes, resulting in coordinatively saturated Ru(II) centers. To estimate the size of the cavity formed by the macrocycle, the distance of C11–C11' is 3.361(5) Å, and the distance of C22–C22' is 10.372(3) Å. The cocrystallized benzene solvent molecules do not form a host–guest complex with **2**, likely because the cavity is inaccessible, as seen in the space-filling model (Figure 2). The protons bound to C11 and C11' are directed inward toward the cavity, while the protons bound to C22 and C22' point outward.

Complex **2** can also be synthesized by the salt metathesis of **KL** and 0.25 equiv of $[\text{RuCp}^*(\mu^3\text{-Cl})_4]$, where complex **2** crystallizes out of the reaction mixture with a different unit cell in the monoclinic $C2/m$ space group with a crystallographically imposed inversion center and mirror plane (see Supporting Information). Interestingly when NaL was used in the salt metathesis instead of **KL**, a different product formed. After a solution of NaL was added dropwise to a solution containing 0.25 equiv of $[\text{RuCp}^*(\mu^3\text{-Cl})_4]$, an orange solution along with a dark precipitate formed after 2 h at RT. The dark precipitate (likely complex **2**, which may have also formed) and NaCl were removed by filtration to give orange complex **3** in the filtrate (Scheme 1). Crystals of **3** were obtained by vapor diffusion of hexanes into a benzene solution (Figure 3). Complex **3** crystallizes in the orthorhombic space group $P2_12_12_1$, where both Cp* and the L^- ligands are coordinated in an η^5 -fashion to Ru(II). In the ^1H NMR spectrum of **3**, the proton at the 9-position of the Ru-bound $\eta^5\text{-L}^-$ resonates as a singlet at 5.12 and 4.81 ppm in CDCl_3 and C_6D_6 , respectively. Complexes **2** and **3** may be viewed as linkage isomers of “ RuCp^*L^- ”, where

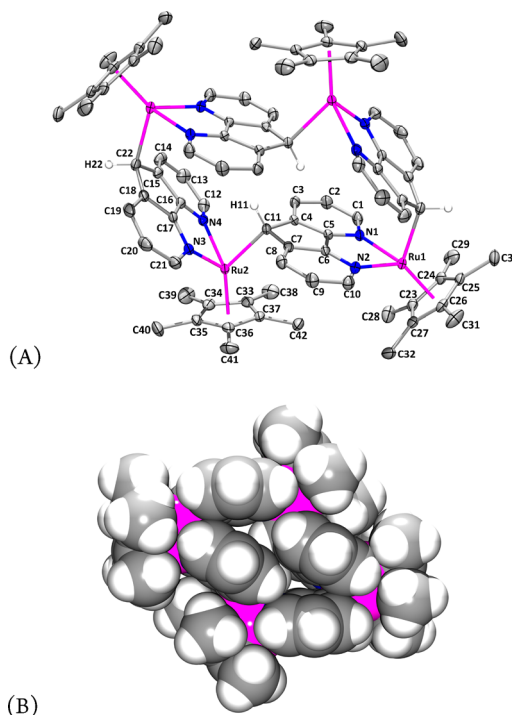


Figure 2. X-ray crystal structure of **2**. (A) Non-hydrogen atoms are shown as 30% probability ellipsoids, and H atoms (except for H11 and H22) are omitted for clarity. (B) Space-filling model of **2**. Selected distances (Å) and angles (deg): Ru1–N1, 2.1683(15); Ru1–N2, 2.1801(15); Ru1–C22, 2.2739(19); Ru1–cent(C23–C27), 1.7854(2); Ru2–N3, 2.1825(15); Ru2–N4, 2.1741(15); Ru2–C11, 2.2626(18); Ru2–cent(C33–C37), 1.7826(2).

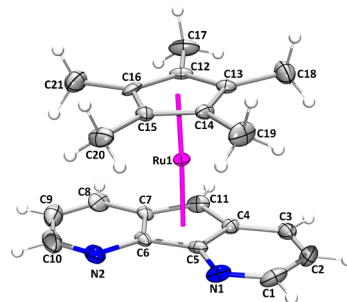


Figure 3. X-ray crystal structure of **3**. Non-hydrogen atoms are shown as 30% probability ellipsoids, and H atoms are shown as spheres of arbitrary radius. Selected distances (Å) and angles (deg): Ru1–cent(C4–C5–C6–C7–C11), 1.85732(16); Ru1–cent(C12–C16), 1.78338(17); cent(C4–C5–C6–C7–C11)–Ru1–cent(C12–C16), 176.41(3).

L^- binds to Ru(II) in either an $\eta^1\text{C}, \kappa^2[\text{N},\text{N}]$ -fashion, giving the tetramer **2**, or an η^5 -fashion, giving the sandwich complex **3**. DFT calculations show that **3** is more stable than **2**. Heating a suspension of complex **2** at 95 °C in C_6D_6 for 1 week only generates a small amount of complex **3** as determined by ^1H NMR spectroscopy, presumably due to the poor solubility of **2**.

Coordination Chemistry of L_pH and L_p^- . The L_pH and L_p^- ligands are multifunctional with a number of potential coordination sites. Previously we demonstrated that metals can bind to L_pH through the N,N-chelate and the phosphine moiety. In addition to these coordination modes L_p^- could also bind Rh(I)¹⁸ or Pt(II)¹⁹ via the P,C-chelate site. The addition of L_pH to 0.25 equiv of $[\text{RuCp}^*(\mu^3\text{-Cl})_4]$ in THF yields orange

X-ray quality crystals of complex **4** after 8 days with slow evaporation (Scheme 2 and Figure 4). Complex **4** is soluble in

Scheme 2. Syntheses of Head-to-Tail Dimeric Macrocycles **4 and **5****

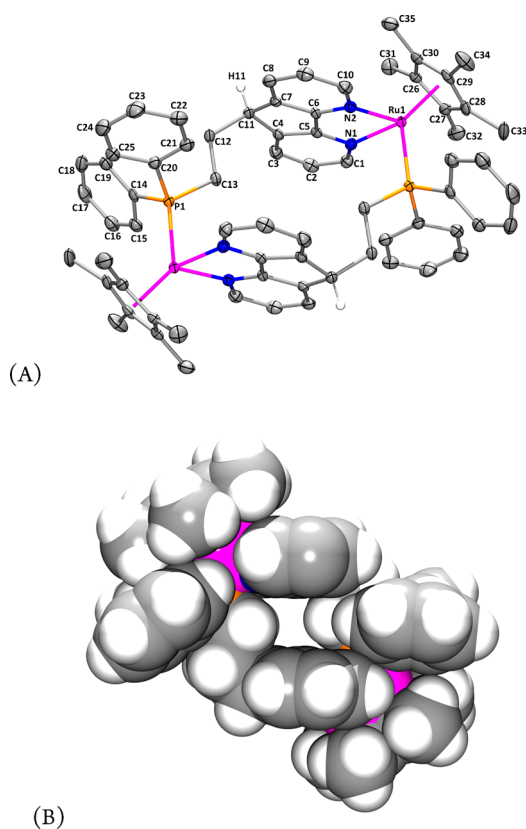
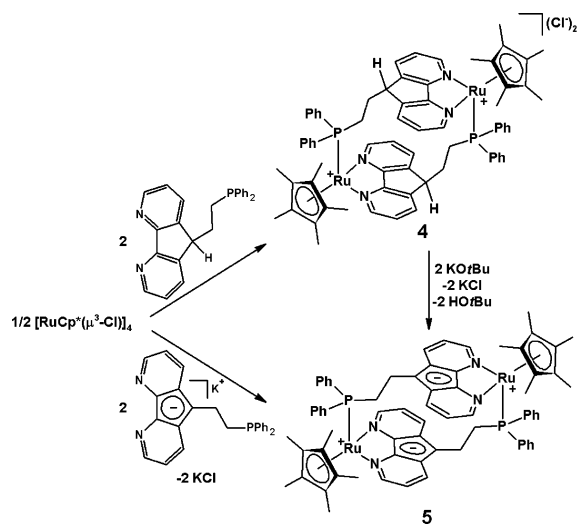


Figure 4. X-ray crystal structure of **4**. (A) Non-hydrogen atoms are shown as 30% probability ellipsoids, and H atoms bound to C11 and C11' are shown as spheres of arbitrary radius. Chloride counterions are omitted for clarity. (B) Space-filling model of dicationic portion of **4**. Selected distances (Å) and angles (deg): Ru1–N1, 2.169(2); Ru1–N2, 2.174(2); Ru1–P1, 2.3151(8); Ru1–cent(C26–C30), 1.8209(2); N1–Ru1–N2, 79.73(9); N1–Ru1–P1, 89.95(7); N2–Ru1–P1, 92.11(6).

DMSO and insoluble in THF, benzene, toluene, hexanes, and pentane. Complex **4** crystallizes in the monoclinic space group

$P2_1/c$ and is a head-to-tail macrocyclic dimer that possesses a crystallographically imposed inversion center in the middle of the cavity. Both the N,N-chelate and phosphine moieties of two separate L_pH ligands coordinatively saturate each of the two pseudo-octahedral $\{RuCp^*\}^+$ vertices. The two diazafluorene moieties are antiparallel, with an interplane separation distance of ~ 5.52 Å. The 1H and ^{31}P NMR spectra are consistent with the dimeric structure being retained in solution. In particular, the ^{31}P NMR spectrum in $DMSO-d_6$ displays a singlet at 37.65 ppm, suggesting that the phosphine remains coordinated to Ru(II). In the 1H NMR spectrum, the protons of the ethylene linker appear as two multiplets at 1.84 and 0.16 ppm, while the proton at the 9-position of the diazafluorene moiety appears as a triplet at 4.16 ppm.

The coordination chemistry of the L_p^- ligand was investigated. A THF solution of KL_p and 0.25 equiv of $[RuCp^*(\mu^3-Cl)]_4$ were allowed to react at RT overnight, giving a brown reaction mixture. The reaction progress was monitored by NMR in C_6D_6 , where the ^{31}P NMR spectrum showed a major peak at 38.02 ppm and minor peaks at ~ 82 , 42.77, and 39.95 ppm. Heating the THF solution at reflux for 9 h did not fully convert the mixture into one species by ^{31}P NMR. Removal of the THF solvent and refluxing the crude mixture in toluene overnight yielded a bright green solution, which has only one singlet at 38.03 ppm, belonging to complex **5** (Scheme 2). Note that the reaction was commenced in THF and there is a switch to toluene; this is because KL_p is insoluble in toluene, and the reaction does not proceed to completion in THF alone. The ^{31}P NMR chemical shift suggests that the phosphine remains coordinated to Ru(II) in solution. In the 1H NMR spectrum, the ethylene protons appear as two multiplets at 2.48 and -0.61 ppm. Complex **5** is soluble in THF, DME, toluene, and benzene, but insoluble in hexanes and pentane. X-ray diffraction quality crystals of **5** were grown from vapor diffusion of hexanes into a benzene solution (Figure 5), or crystals of $5 \cdot (\text{pentane})$ were grown from vapor diffusion of pentane into a DME solution (see Supporting Information). Crystals of **5** grown from benzene–hexanes crystallized in the monoclinic space group $P2_1/n$; molecules of **5** do not possess a crystallographically imposed inversion center, and the dihedral angle between the two diazafluorenyl moieties is $\sim 13^\circ$ within

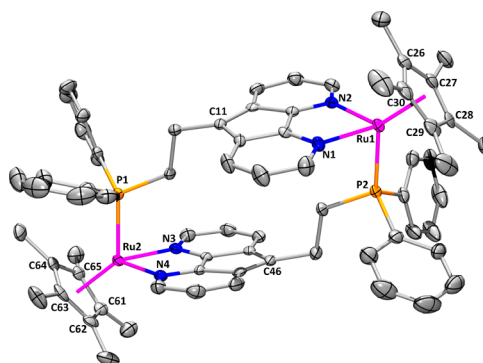
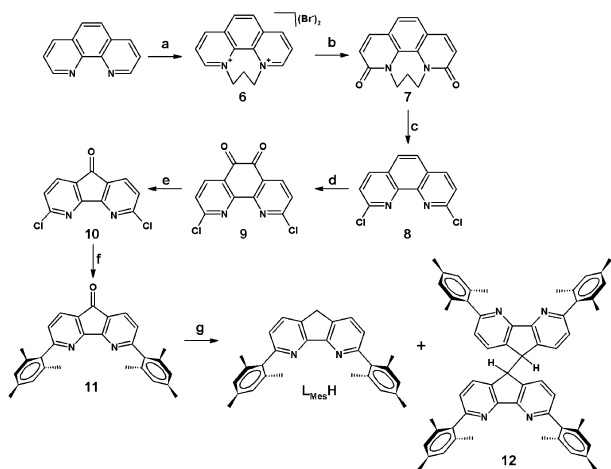


Figure 5. X-ray crystal structure of **5**. (A) Non-hydrogen atoms are shown as 30% probability ellipsoids, and H atoms are omitted for clarity. Selected distances (Å) and angles (deg): Ru1–N1, 2.171(3); Ru1–N2, 2.197(3); Ru1–P2, 2.3302(9); Ru1–cent(C26–C30), 1.8155(3); Ru2–N3, 2.178(3); Ru2–N4, 2.180(3); Ru2–P1, 2.3260(9); Ru2–cent(C61–C65), 1.8103(3); N1–Ru1–N2, 80.18(10); N1–Ru1–P2, 86.81(7); N2–Ru1–P2, 88.85(7); N3–Ru2–N4, 80.46(10); N3–Ru2–P1, 90.44(7); N4–Ru2–P1, 85.36(7).

one molecule of **5**. Crystals of **5** (pentane) crystallize in the triclinic space group $P\bar{1}$, with a crystallographically imposed inversion center in the middle of the molecule, and therefore, the diazafluorenyl moieties within one molecule are antiparallel. The intramolecular separation distances between the diazafluorenyl moieties are ~ 4.80 and 4.69 Å for the two independent molecules of **5**, respectively. Complex **5** can also be prepared by the deprotonation of complex **4** with KOtBu (Scheme 2). The advantage of this route is that it does not require a change of solvent during the preparation.

L_pH and L_p^- both possess an N,N-chelate site and a phosphine moiety at the opposite end of the ligand framework. Similar to what has been reported previously in the literature of coordination-driven self-assembly with ditopic ambidentate ligands,^{1,5,6} despite the possible formation of constitutional isomers and oligomers, a single head-to-tail isomer of **4** or **5** forms cleanly. A head-to-head isomer does not seem to be thermodynamically favored.

Synthesis of $L_{Mes}H$. We envisioned that aryl groups could be installed onto the 4,5-diazafluorene framework at the 3- and 6-positions via Suzuki coupling. The synthesis of 3,6-dimesityl-4,5-diazafluorene ($L_{Mes}H$) from 1,10-phenanthroline is shown in Scheme 3. 1,10-Phenanthroline is first protected with excess

Scheme 3^a

^aConditions: (a) Excess 1,3-dibromopropane, toluene, 110 °C, 4 h (90% yield);^{61,62} (b) excess KOtBu, HOtBu, 45 °C (83% yield);⁶² (c) POCl₃, PCl₅, 110 °C, 8 h (88% yield);^{61,62} (d) H₂SO₄, HNO₃, KBr, 0 to 80 °C, 3 h (71% yield);⁶¹ (e) step 1: 2.38 equiv KOH, 100 °C, 10 min; step 2: 0.75 equiv KMnO_{4(aq)} slow addition, 100 °C overnight (63% yield); (f) 3 equiv 2,4,6-trimethylphenylboronic acid, 21.5 equiv Na₂CO₃, 8.4 mol % Pd(PPh₃)₄, toluene–H₂O (2:1), 115 °C, overnight (95% yield); (g) hydrazine hydrate, 180 °C, 7.5 h (75% yield of $L_{Mes}H$, 12% yield of **12**) or overnight (92% yield of $L_{Mes}H$).

1,3-dibromopropane in refluxing toluene. Toluene was used as the solvent for this reaction as opposed to the higher boiling and more toxic nitrobenzene,⁶¹ or chlorobenzene,⁶² used in the literature, and the N,N-protected product **6** could be isolated in 90% yield. The oxidation of **6** initially proved to be the bottleneck in the earlier steps of the synthetic route. Previously we performed this oxidation using [K₃Fe(CN)₆] in basic aqueous solution.⁶¹ Even with an optimized workup involving neutralization with HBr and liquid–liquid extraction (that forgoes a tedious Soxhlet extraction) the best yield obtained was 45%, and the largest manageable scale in our hands only produced ~ 15 g of desired product **7**. Guo and co-workers have

recently reported that the oxidation of **6** could be carried out with excess KOtBu in HOtBu in air.⁶² We found that Guo's reaction is higher yielding, less time-consuming, and highly scalable; 216 g of the oxidation product **7** could be isolated in 83% yield in one batch. The reaction of compound **7** with PCl₅ and POCl₃ gave 2,9-dichloro-1,10-phenanthroline (**8**) in 88% yield, comparable to the literature.^{61,62}

It is worth noting that **LH** is prepared in two steps from 1,10-phenanthroline: an oxidative ring contraction with KOH and KMnO₄ and a subsequent Wolff–Kishner reduction of the resulting 4,5-diazafluorene-9-one.^{58,59} The oxidative ring contraction of **8** with analogous reaction conditions was unsuccessful; only a trace of the desired 3,6-dichloro-4,5-diazafluorene-9-one (**10**) could be observed by NMR, likely due to the limited solubility of **8** in water. The oxidative ring contraction of 1,10-phenanthroline likely proceeds via a phenanthrolinequinone intermediate.^{58,74} Therefore, we decided to explore whether a ring contraction of 2,9-dichloro-1,10-phenanthroline-5,6-dione (**9**) would give the desired compound **10**. The oxidation of compound **8** was carried out with KBr and HNO₃ in concentrated sulfuric acid; after workup a 71% yield of dione **9** was obtained, similar to the literature.⁶¹

The rapid benzylic acid rearrangement and decarboxylation of **9** can be carried out by reacting **9** with KOH in refluxing H₂O. The subsequent oxidation by a slow addition of a dilute and warm solution of KMnO₄ gives the desired product **10** in 63% yield. The ¹H NMR spectrum of **10** in CDCl₃ has two doublets at 7.95 and 7.43 ppm, similar to the starting material **9**, which shows two doublets at 8.44 and 7.62 ppm. X-ray quality crystals of **10** were obtained from vapor diffusion of pentane into a CHCl₃ solution, and crystallography revealed that indeed the ring contraction had occurred, corroborating the GC-MS information (Figure 6). Compound **10** crystallizes in the

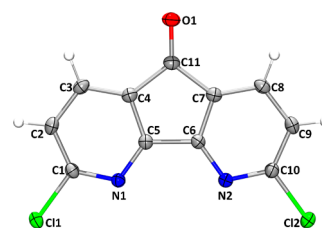


Figure 6. X-ray crystal structure of **10**. Non-hydrogen atoms are shown as 30% probability ellipsoids, and H atoms are shown as spheres of arbitrary radius.

monoclinic space group $P2_1/c$ as a planar molecule. In the solid state compound **10** engages in dihalogen bonding, where the short contact distance between Cl1 and Cl1' of an adjacent molecule is ~ 3.38 Å. The Suzuki coupling reaction of compound **10** with 2,4,6-trimethylphenylboronic acid in toluene in the presence of aqueous Na₂CO₃ and Pd(PPh₃)₄ (8.4 mol % vs compound **10**) proceeded straightforwardly, where compound **11** was obtained in 95% yield after column chromatography. Compound **11** exhibits bright yellow luminescence in the solid state and in solution when irradiated with 365 nm UV light.

The Wolff–Kishner reduction of compound **11** was accomplished with hydrazine hydrate at 180 °C in a sealed stainless steel bomb. However a difference in the yields and selectivity of the reaction was observed depending on the amount of compound **11** per volume of hydrazine hydrate and the reaction time at 180 °C. When a larger amount of **11** was

reacted for a shorter period of time (570 mg of **11** with 12 mL of hydrazine hydrate for 7.5 h), two spots exhibiting bright blue luminescence under 365 nm UV irradiation were observed on the TLC plate. The desired 3,6-dimesityl-4,5-diazafluorene ($L_{\text{Mes}}\text{H}$) with a higher R_f was isolated in 75% yield, while 9,9'-bi-3,6-dimesityl-4,5-diazafluorenyl (**12**) with a lower R_f was isolated in 12% yield. When a smaller amount of **11** was reacted for a longer time (360 mg of **11** with 12 mL of hydrazine hydrate overnight), $L_{\text{Mes}}\text{H}$ could be isolated in 92% yield without the formation of the **12** byproduct. Several peaks of the ^1H NMR spectrum of **12** are broad including those belonging to the two *ortho* methyl groups of each of the mesityl substituents and the pyridyl protons.

Crystals of $L_{\text{Mes}}\text{H}$ were obtained by diffusion of hexanes into a toluene solution (Figure 7), and crystals of **12** were obtained

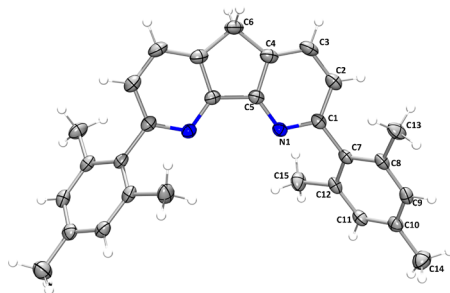


Figure 7. X-ray crystal structure of $L_{\text{Mes}}\text{H}$. Non-hydrogen atoms are shown as 30% probability ellipsoids, and H atoms are shown as spheres of arbitrary radius.

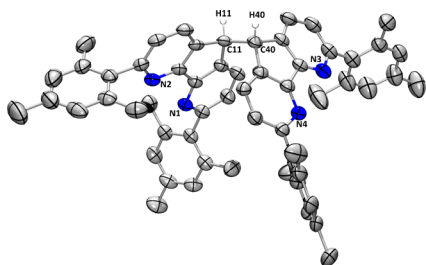


Figure 8. X-ray crystal structure of **12**. Non-hydrogen atoms are shown as 30% probability ellipsoids, and H atoms bound to C11 and C40 are shown as spheres of arbitrary radius.

by diffusion of Et_2O into a CHCl_3 solution (Figure 8). $L_{\text{Mes}}\text{H}$ crystallizes in the orthorhombic space group $Pbcn$ with crystallographically imposed C_2 symmetry bisecting the molecule. The angle between the plane defined by the diazafluorene moiety and the plane defined by the mesityl moiety is $\sim 57^\circ$. Compound **12** crystallizes in the trigonal space group $P3_2$ and adopts a *gauche* conformation about the bond linking the two 3,6-dimesityl-4,5-diazafluorenyl moieties. The $\text{H11}-\text{C11}-\text{C40}-\text{H40}$ torsion angle in **12** is $59.10(5)^\circ$, and the length of the $\text{C11}-\text{C40}$ bond is $1.565(9)$ Å, similar to 9,9'-bi-4,5-diazafluorenyl, where a *gauche* conformation has also been established by X-ray crystallography.⁷⁵

Coordination Chemistry of $L_{\text{Mes}}\text{H}$ and L_{Mes}^- . With the $L_{\text{Mes}}\text{H}$ ligand in hand we decided to probe its coordination chemistry. The addition of $L_{\text{Mes}}\text{H}$ to 0.25 equiv of $[\text{RuCp}^*(\mu^3\text{-Cl})_4]$ in THF gradually yielded colorless X-ray quality crystals of **13** over one week (Scheme 4 and Figure 9). Complex **13** is

Scheme 4. Syntheses of Linkage Isomers **14** and **15**

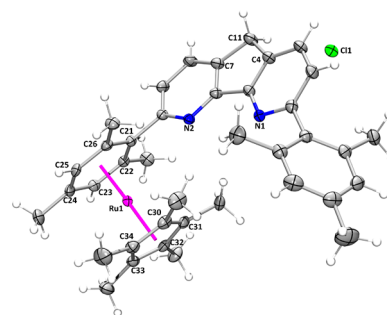
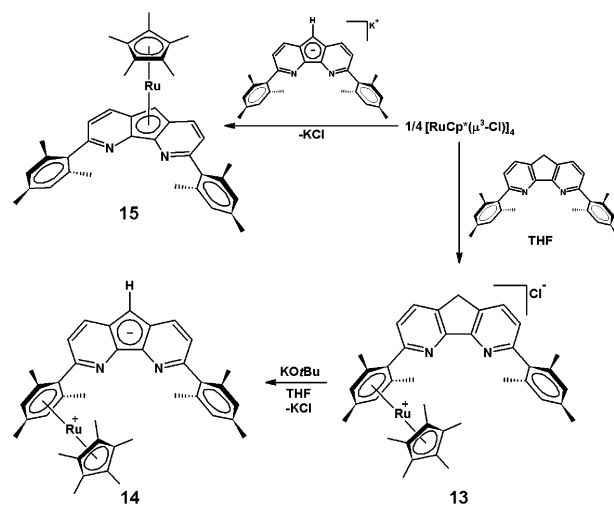


Figure 9. X-ray crystal structure of **13**. Non-hydrogen atoms are shown as 30% probability ellipsoids, and H-atoms are shown as spheres of arbitrary radius. The cocrystallized THF solvent molecule is omitted for clarity. Selected distances (Å) and angles (deg): $\text{C4}-\text{C11}$, 1.505(3); $\text{C7}-\text{C11}$, 1.509(3); $\text{Ru1}-\text{cent}(\text{C21}-\text{C26})$, 1.70914(18); $\text{Ru1}-\text{cent}(\text{C30}-\text{C34})$, 1.81304(19); $\text{C4}-\text{C11}-\text{C7}$, 102.30(17); $\text{cent}(\text{C21}-\text{C26})-\text{Ru1}-\text{cent}(\text{C30}-\text{C34})$, 178.607(10).

soluble in DMSO, slightly soluble in THF, DME, benzene, toluene, and diethyl ether, and insoluble in hexanes and pentane. Complex **13** crystallizes in the triclinic space group $P\bar{1}$, where one of the mesityl rings coordinates to the $\{\text{RuCp}^*\}^+$ fragment in an η^6 -fashion. The chloride is no longer bound to the Ru center, and the N,N-chelate site of $L_{\text{Mes}}\text{H}$ remains unoccupied. The steric bulk of the $L_{\text{Mes}}\text{H}$ and Cp^* ligands, along with the known affinity of the $\{\text{RuCp}^*\}^+$ fragment for π -aromatic ligands,⁶⁰ likely prevented κ^2 -[N,N] coordination in complex **13**, as opposed to what is observed in complex **1**, with a less sterically demanding LH ligand. The dihedral angle between the diazafluorene and the uncoordinated mesityl substituent planes is $\sim 52^\circ$, while the dihedral angle between the diazafluorene and the coordinated mesityl planes is $\sim 60^\circ$. It is also worth noting that the $\{\text{RuCp}^*\}^+$ moiety points inward toward the nitrogen chelate, rather than outward, which would minimize steric repulsion from the Cp^* . The ^1H NMR spectrum in $\text{DMSO}-d_6$ revealed an unsymmetrical structure in solution: four sets of pyridyl C-H peaks and two inequivalent mesityl substituents. The two aromatic protons on the $\text{Ru}(\text{II})$ -bound mesityl substituent are significantly upfield shifted to 5.89 ppm, compared to the protons on the dangling mesityl substituent at 6.95 ppm. The methylene protons at the 9-position of the diazafluorene moiety resonate as a singlet at 4.14 ppm.

Complex **13** can be deprotonated with KO t Bu to give the red zwitterionic complex **14**. Complex **14** is soluble in DMSO and THF, but insoluble in toluene, benzene, DME, hexanes, and pentane. Layering a THF solution of complex **14** with toluene resulted in the formation of X-ray quality crystals (Figure 10).

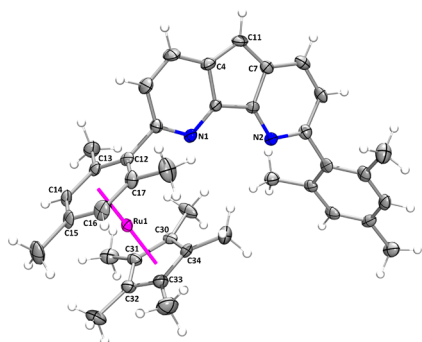


Figure 10. X-ray crystal structure of **14**. Non-hydrogen atoms are shown as 30% probability ellipsoids, and H atoms are shown as spheres of arbitrary radius. Selected distances (Å) and angles (deg): C4–C11, 1.404(5); C7–C11, 1.403(5); Ru1–cent(C12–C17), 1.7084(3); Ru1–cent(C30–C34), 1.8111(3); C4–C11–C7, 107.2(3); cent(C12–C17)–Ru1–cent(C30–C34), 179.08(2).

Complex **14** crystallizes in the monoclinic space group $P2_1/c$, where complex **14** is structurally analogous to the complex cation of **13**. The Ru(II) center remains coordinated to the arene. The 9-position of the diazafluorene moiety had been deprotonated, as evidenced by the bond lengths and angles about the backbone carbon and absence of chloride counterion. The C4–C11–C7 angle in complex **13** is 102.30(17)°, while after deprotonation the C4–C11–C7 angle in complex **14** is 107.2(3)°. The dihedral angle between the diazafluorenyl and the uncoordinated mesityl planes is ~63°, while the dihedral angle between the diazafluorenyl and the coordinated mesityl planes is ~86°. Similar to complex **13**, the ^1H NMR spectrum of complex **14** in DMSO- d_6 is also unsymmetrical, where most of the aromatic protons are downfield shifted compared to the corresponding protons in complex **13**. The proton at the 9-position of the anionic L_{Mes}^- ligand in complex **14** appears as a singlet at 5.93 ppm, suggesting the aromaticity of the central C_5 -ring.

Different linkage isomers of $[\text{RuCp}^*\text{L}_{\text{Mes}}]$ can be produced depending on the reaction sequence. If the Ru-bound neutral $\text{L}_{\text{Mes}}\text{H}$ ligand was deprotonated, the Ru(II) center is coordinated to the arene; however, if L_{Mes}^- is added to Ru(II) directly, then the $\{\text{RuCp}^*\}^+$ unit is coordinated to the central C_5 -ring. $\text{L}_{\text{Mes}}\text{H}$ can be deprotonated with KO t Bu in THF to give a deep red solution of KL_{Mes} . When KL_{Mes} was reacted with 0.25 equiv of $[\text{RuCp}^*(\mu^3\text{-Cl})_4]$, a bright orange metallocene complex **15** was isolated (Scheme 4). Complex **15** is soluble in THF, DME, toluene, benzene, DCM, and chloroform, slightly soluble in DMSO, and insoluble in Et $_2$ O, hexanes, and pentane. Crystals of $15 \cdot (\text{C}_6\text{H}_6)$ were obtained by vapor diffusion of hexanes into a benzene solution (Figure 11); analogously crystals of $15 \cdot (\text{Et}_2\text{O})$ were grown by vapor diffusion of diethyl ether into a THF solution (see Supporting Information). Complex **15** crystallizes in the monoclinic space group $P2_1/c$ as a benzene solvate, where both Cp^* and L_{Mes}^- ligands are coordinated in an η^5 -fashion to Ru(II). The dihedral angles between the diazafluorenyl plane and each mesityl ring are 66.39° and 55.03°, respectively. The metallocene is slightly

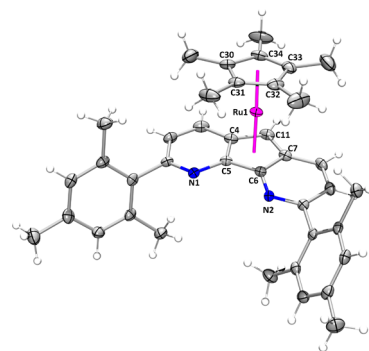


Figure 11. X-ray crystal structure of $15 \cdot (\text{C}_6\text{H}_6)$. Non-hydrogen atoms are shown as 30% probability ellipsoids, and H atoms are shown as spheres of arbitrary radius. The cocrystallized benzene solvent molecule is omitted for clarity. Selected distances (Å) and angles (deg): Ru1–cent(C4–C5–C6–C7–C11), 1.86492(18); Ru1–cent(C30–C34), 1.78074(18); cent(C4–C5–C6–C7–C11)–Ru1–cent(C30–C34), 176.641(12).

bent, with the centroid(C_5 -ring of Cp^*)–Ru–centroid(C_5 -ring of diazafluorenyl) angle of ~177°. Analogously, complex **15** crystallizes in the monoclinic space group $P2_1/n$ as its diethyl ether solvate. The ^1H NMR spectrum in CDCl_3 revealed a symmetrical structure in solution, where the 2,6-methyl groups on the mesityl substituents appear as a broad singlet at 2.18 ppm, indicating that the mesityl groups can slowly rotate at RT and are not locked. The chemical shift of the backbone proton at the 9-position of the L_{Mes}^- ligand appears at 5.12 ppm. A related sandwich-type complex of CoCp^* with 4,5-diazafluorenone has been reported.⁷⁶ The selectivity of this reaction for the η^5 - over the κ^2 -[N,N] coordination mode is likely governed by sterics. While the less bulky L^- can coordinate through both the N- and C-donors, the steric bulk of L_{Mes}^- precludes the κ^2 -[N,N] coordination mode. In contrast β -diiminate ligands (monoanionic N-chelate ligands analogous to L_{Ar}^-) coordinate to Ru half-sandwich fragments through the κ^2 -[N,N] coordination mode.^{24,77–79} Another example of linkage isomers from the literature with a ligand that possesses both a cyclopentadienyl moiety and an aryl ring was reported by Masters and co-workers.⁸⁰ The bulky cyclopentadienyl derivative (C_5Ph_5) $^-$ forms two linkage isomers with Fe(II): the conventional metallocene $[\text{Fe}(\eta^5\text{-C}_5\text{Ph}_5)_2]$ and the linkage isomers $[\text{Fe}(\eta^5\text{-C}_5\text{Ph}_5)\{(\eta^{5/6}\text{-C}_6\text{H}_5)(\text{C}_5\text{Ph}_4)\}]$. The crystal structure of $[\text{Fe}(\eta^5\text{-C}_5\text{Ph}_5)\{(\eta^{5/6}\text{-C}_6\text{H}_5)(\text{C}_5\text{Ph}_4)\}]$ revealed a mixture of two similar yet independent molecules in the unit cell, where one of the phenyl rings is bound in either an η^5 - or an η^6 -fashion to the iron center.⁸⁰ Thermodynamically **15** is 9.1 kcal·mol $^{-1}$ more stable than **14**, as determined by DFT. Heating **14** at 110 °C in DMSO- d_6 overnight does not result in any conversion to complex **15** by ^1H NMR spectroscopy.

CONCLUSIONS

In summary, we have shown the utility of diazafluorene derivatives as ligands in the assembly of linkage isomers and macrocycles. The rich coordination chemistry of the $\{\text{RuCp}^*\}^+$ fragment was extended to the ambidentate LH/L^- , $\text{L}_p\text{H}/\text{L}_p^-$, and $\text{L}_{\text{Mes}}\text{H}/\text{L}_{\text{Mes}}^-$ ligand families. The L^- ligand can coordinate through both the N-donors and the C-donor simultaneously to form the tetrameric macrocyclic complex **2**; it also can coordinate in an η^5 -fashion exclusively to form the sandwich complex **3**. The head-to-tail macrocyclic dimers were formed with either L_pH or L_p^- ligands, giving complexes **4** and **5**,

respectively. The synthesis of the $L_{\text{Mes}}\text{H}$ ligand with mesityl groups installed *ortho* to the N-donors was achieved in a scalable manner. These newly installed mesityl groups within the $L_{\text{Mes}}\text{H}$ ligand framework provided an additional arene coordination site. The sterically bulky $L_{\text{Mes}}\text{H}$ ligand coordinated to the $\{\text{RuCp}^*\}^+$ fragment through the arene coordination site, furnishing complex **13**, which can be deprotonated to form the zwitterionic complex **14**. When the reaction sequence was changed, the linkage isomer, sandwich complex **15**, formed. Current efforts are focused on utilizing the monomeric RuCp^* complexes as redox-active metalloligands to generate bimetallic complexes for small-molecule activation and catalysis, as well as extending the β -diiminato analog of L_{Ar}^- to include bulkier aryl groups and other metals.

■ ASSOCIATED CONTENT

■ Supporting Information

NMR spectra, GC chromatograms, and MS spectra, DFT-optimized geometry coordinates of **2**, **3**, **14**, and **15**; crystallographic data tables and CIF files for **1**, **2**, **2**· $2(\text{C}_6\text{H}_6)$, **3**, **4**, **5**, **5**·(pentane), **10**, $L_{\text{Mes}}\text{H}$, **12**, **13**·(THF), **14**, **15**· (C_6H_6) , and **15**· (Et_2O) . This material is available free of charge via the Internet at <http://pubs.acs.org>.

■ AUTHOR INFORMATION

■ Corresponding Author

*E-mail: dsong@chem.utoronto.ca.

■ Notes

The authors declare no competing financial interest.

■ ACKNOWLEDGMENTS

We thank the Natural Science and Engineering Research Council of Canada (NSERC) for funding. V.T.A. gratefully thanks the NSERC for a postgraduate scholarship (PGS D2) and the government of Ontario for an Ontario Graduate Scholarship (OGS). The authors also wish to acknowledge the Canadian Foundation for Innovation Project no. 19119 and the Ontario Research Fund for funding the CSICOMP NMR lab at the University of Toronto, enabling the purchase of several new spectrometers.

■ REFERENCES

- (1) Northrop, B. H.; Zheng, Y.; Chi, K.; Stang, P. J. *Acc. Chem. Res.* **2009**, *42*, 1554–1563.
- (2) Swiegers, G.; Malefetse, T. *Chem. Rev.* **2000**, *100*, 3483–3537.
- (3) Sloan, T. E.; Busch, D. H. *Inorg. Chem.* **1978**, *17*, 2043–2047.
- (4) Fujita, M.; Tominaga, M.; Hori, A.; Therrien, B. *Acc. Chem. Res.* **2005**, *38*, 369–378.
- (5) Chi, K.; Addicott, C.; Arif, A.; Stang, P. J. *Am. Chem. Soc.* **2004**, *126*, 16569–16574.
- (6) Jung, H.; Dubey, A.; Koo, H. J.; Vajpayee, V.; Cook, T. R.; Kim, H.; Kang, S. C.; Stang, P. J.; Chi, K. *Chem.—Eur. J.* **2013**, *19*, 6709–6717.
- (7) Han, Y.; Jia, W.; Yu, W.; Jin, G. *Chem. Soc. Rev.* **2009**, *38*, 3419–3434.
- (8) Khoshbin, M.; Ovchinnikov, M.; Mirkin, C.; Zakharov, L.; Rheingold, A. *Inorg. Chem.* **2005**, *44*, 496–501.
- (9) Barry, N. P. E.; Furrer, J.; Freudenreich, J.; Suess-Fink, G.; Therrien, B. *Eur. J. Inorg. Chem.* **2010**, 725–728.
- (10) Mirtschin, S.; Slabon-Turski, A.; Scopelliti, R.; Velders, A. H.; Severin, K. *J. Am. Chem. Soc.* **2010**, *132*, 14004–14005.
- (11) Vajpayee, V.; Song, Y. H.; Cook, T. R.; Kim, H.; Lee, Y.; Stang, P. J.; Chi, K. *J. Am. Chem. Soc.* **2011**, *133*, 19646–19649.

- (12) Vajpayee, V.; Song, Y. H.; Yang, Y. J.; Kang, S. C.; Cook, T. R.; Kim, D. W.; Lah, M. S.; Kim, I. S.; Wang, M.; Stang, P. J.; Chi, K. *Organometallics* **2011**, *30*, 6482–6489.
- (13) Jiang, H.; Song, D. *Organometallics* **2008**, *27*, 3587–3592.
- (14) Jiang, H.; Stepowska, E.; Song, D. *Eur. J. Inorg. Chem.* **2009**, 2083–2089.
- (15) Jiang, H.; Stepowska, E.; Song, D. *Dalton Trans.* **2008**, 5879–5881.
- (16) Stepowska, E.; Jiang, H.; Song, D. *Chem. Commun.* **2010**, 46, 556–558.
- (17) Annibale, V. T.; Song, D. *Chem. Commun.* **2012**, 48, 5416–5418.
- (18) Tan, R.; Chiu, F. S. N.; Hadzovic, A.; Song, D. *Organometallics* **2012**, *31*, 2184–2192.
- (19) Batcup, R.; Chiu, F. S. N.; Annibale, V. T.; Huh, J.-E. U.; Tan, R.; Song, D. *Dalton Trans.* **2013**, DOI: 10.1039/C3DT52135D.
- (20) For reviews on β -diiminato chemistry see: (a) Bourget-Merle, L.; Lappert, M. F.; Severn, J. *Chem. Rev.* **2002**, *102*, 3031. (b) Mindiola, D. J. *Angew. Chem., Int. Ed.* **2009**, *48*, 6198. (c) Holland, P. L. *Acc. Chem. Res.* **2008**, *41*, 905. (d) Roesky, H. W.; Singh, S.; Jancik, V.; Chandrasekhar, V. *Acc. Chem. Res.* **2004**, *37*, 969. (e) Piers, W. E.; Emslie, D. J. H. *Coord. Chem. Rev.* **2002**, *131*, 233–234. (f) Zhu, D.; Budzelaar, P. H. M. *Dalton Trans.* **2013**, 42, 11343–11354.
- (21) Annibale, V. T.; Lund, L. M.; Song, D. *Chem. Commun.* **2010**, 46, 8261–8263.
- (22) Annibale, V. T.; Tan, R.; Janetzko, J.; Lund, L. M.; Song, D. *Inorg. Chim. Acta* **2012**, *380*, 308–321.
- (23) Ferro, L.; Coles, M. P.; Day, I. J.; Fulton, J. R. *Organometallics* **2010**, *29*, 2911–2915.
- (24) Phillips, A. D.; Laurenczy, G.; Scopelliti, R.; Dyson, P. J. *Organometallics* **2007**, *26*, 1120–1122.
- (25) Hadzovic, A.; Song, D. *Organometallics* **2008**, *27*, 1290–1298.
- (26) Scheuermann, M. L.; Fekl, U.; Kaminsky, W.; Goldberg, K. I. *Organometallics* **2010**, *29*, 4749–4751.
- (27) Scheuermann, M. L.; Luedtke, A. T.; Hanson, S. K.; Fekl, U.; Kaminsky, W.; Goldberg, K. I. *Organometallics* **2013**, *32*, 4752–4758.
- (28) Bailey, P. J.; Melchionna, M.; Parsons, S. *Organometallics* **2007**, *26*, 128–135.
- (29) Enk, B.; Eisenstecken, D.; Kopacka, L.; Wurst, K.; Mueller, T.; Pevny, F.; Winter, R. F.; Bildstein, B. *Organometallics* **2010**, *29*, 3169–3178.
- (30) Bailey, P. J.; Rahman, M.; Parsons, S.; Azhar, M. R.; White, F. J. *Dalton Trans.* **2013**, 42, 2879–2886.
- (31) Okuda, J. *Top. Curr. Chem.* **1992**, *160*, 97–145.
- (32) Bercaw, J. E.; Bell, L. G.; Brintzin, H. H.; Marvich, R. H. *J. Am. Chem. Soc.* **1972**, *94*, 1219–1238.
- (33) Manriquez, J. M.; Bercaw, J. E. *J. Am. Chem. Soc.* **1974**, *96*, 6229–6230.
- (34) van Asselt, A.; Burger, B. J.; Gibson, V. C.; Bercaw, J. E. *J. Am. Chem. Soc.* **1986**, *108*, 5347–5349.
- (35) Evans, W. J.; Hughes, L. A.; Hanusa, T. P. *J. Am. Chem. Soc.* **1984**, *106*, 4270–4272.
- (36) Manriquez, J. M.; Fagan, P. J.; Marks, T. J. *J. Am. Chem. Soc.* **1978**, *100*, 3939–3941.
- (37) Mork, B. V.; Tilley, T. D. *J. Am. Chem. Soc.* **2004**, *126*, 4375–4385.
- (38) Resa, I.; Carmona, E.; Gutierrez-Puebla, E.; Monge, A. *Science* **2004**, *305*, 1136–1138.
- (39) Jutzki, P.; Reumann, G. *J. Chem. Soc., Dalton Trans.* **2000**, 2237–2244.
- (40) Campion, B. K.; Heyn, R. H.; Tilley, T. D. *J. Chem. Soc., Chem. Commun.* **1992**, 1201–1203.
- (41) Campion, B. K.; Heyn, R. H.; Tilley, T. D.; Rheingold, A. L. *J. Am. Chem. Soc.* **1993**, *115*, 5527–5537.
- (42) Dysard, J. M.; Tilley, T. D. *Organometallics* **2000**, *19*, 4726–4732.
- (43) Loren, S. D.; Campion, B. K.; Heyn, R. H.; Tilley, T. D.; Bursten, B. E.; Luth, K. W. *J. Am. Chem. Soc.* **1989**, *111*, 4712–4718.

- (44) Mork, B. V.; McMillan, A.; Yuen, H.; Tilley, T. D. *Organometallics* **2004**, *23*, 2855–2859.
- (45) Tilley, T. D.; Grubbs, R. H.; Bercaw, J. E. *Organometallics* **1984**, *3*, 274–278.
- (46) Johnson, T. J.; Huffman, J. C.; Caulton, K. G. *J. Am. Chem. Soc.* **1992**, *114*, 2725–2726.
- (47) Johnson, T. J.; Coan, P. S.; Caulton, K. G. *Inorg. Chem.* **1993**, *32*, 4594–4599.
- (48) Johnson, T. J.; Folting, K.; Streib, W. E.; Martin, J. D.; Huffman, J. C.; Jackson, S. A.; Eisenstein, O.; Caulton, K. G. *Inorg. Chem.* **1995**, *34*, 488–499.
- (49) Kuhlman, R.; Streib, K.; Caulton, K. G. *J. Am. Chem. Soc.* **1993**, *115*, 5813–5814.
- (50) Kuhlman, R.; Folting, K.; Caulton, K. G. *Organometallics* **1995**, *14*, 3188–3195.
- (51) Rankin, M. A.; McDonald, R.; Ferguson, M. J.; Stradiotto, M. *Angew. Chem., Int. Ed.* **2005**, *44*, 3603–3606.
- (52) Rankin, M. A.; McDonald, R.; Ferguson, M. J.; Stradiotto, M. *Organometallics* **2005**, *24*, 4981–4994.
- (53) Rankin, M. A.; Hesp, K. D.; Schatte, G.; McDonald, R.; Stradiotto, M. *Dalton Trans.* **2009**, 4756–4765.
- (54) Rankin, M. A.; Hesp, K. D.; Schatte, G.; McDonald, R.; Stradiotto, M. *Chem. Commun.* **2008**, 250–252.
- (55) Rankin, M. A.; MacLean, D. F.; McDonald, R.; Ferguson, M. J.; Lumsden, M. D.; Stradiotto, M. *Organometallics* **2009**, *28*, 74–83.
- (56) Rankin, M. A.; Schatte, G.; McDonald, R.; Stradiotto, M. *Organometallics* **2008**, *27*, 6286–6299.
- (57) Lundgren, R. J.; Rankin, M. A.; McDonald, R.; Stradiotto, M. *Organometallics* **2008**, *27*, 254–258.
- (58) Plater, M.; Kemp, S.; Lattmann, E. *J. Chem. Soc., Perkin Trans. 1* **2000**, 971–979.
- (59) Thummel, R. P.; Lefoulon, F.; Mahadevan, R. *J. Org. Chem.* **1985**, *50*, 3824–3828.
- (60) Fagan, P. J.; Ward, M. D.; Calabrese, J. C. *J. Am. Chem. Soc.* **1989**, *111*, 1698–1719.
- (61) Frey, J.; Kraus, T.; Heitz, V.; Sauvage, J. *Chem.—Eur. J.* **2007**, *13*, 7584–7594.
- (62) Guo, H. C.; Zheng, R. H.; Jiang, H. J. *Org. Prep. Proced. Int.* **2012**, *44*, 392–396.
- (63) Apex 2 Software Package; Bruker AXS Inc., 2013.
- (64) (a) Sheldrick, G. M. *Acta Crystallogr., Sect. A: Found. Crystallogr.* **2008**, *64*, 112. (b) <http://shelx.uni-ac.gwdg.de/SHELX/index.php>.
- (65) Spek, A. L. *J. Appl. Crystallogr.* **2003**, *36*, 7.
- (66) Frisch, M. J.; Trucks, G. W.; Schlegel, H. B.; Scuseria, G. E.; Robb, M. A.; Cheeseman, J. R.; Scalmani, G.; Barone, V.; Mennucci, B.; Petersson, G. A.; Nakatsuji, H.; Caricato, M.; Li, X.; Hratchian, H. P.; Izmaylov, A. F.; Bloino, J.; Zheng, G.; Sonnenberg, J. L.; Hada, M.; Ehara, M.; Toyota, K.; Fukuda, R.; Hasegawa, J.; Ishida, M.; Nakajima, T.; Honda, Y.; Kitao, O.; Nakai, H.; Vreven, T.; Montgomery, J. A., Jr.; Peralta, J. E.; Ogliaro, F.; Bearpark, M.; Heyd, J. J.; Brothers, E.; Kudin, K. N.; Staroverov, V. N.; Keith, T.; Kobayashi, R.; Normand, J.; Raghavachari, K.; Rendell, A.; Burant, J. C.; Iyengar, S. S.; Tomasi, J.; Cossi, M.; Rega, N.; Millam, J. M.; Klene, M.; Knox, J. E.; Cross, J. B.; Bakken, V.; Adamo, C.; Jaramillo, J.; Gomperts, R.; Stratmann, R. E.; Yazyev, O.; Austin, A. J.; Cammi, R.; Pomelli, C.; Ochterski, J. W.; Martin, R. L.; Morokuma, K.; Zakrzewski, V. G.; Voth, G. A.; Salvador, P.; Dannenberg, J. J.; Dapprich, S.; Daniels, A. D.; Farkas, O.; Foresman, J. B.; Ortiz, J. V.; Cioslowski, J.; Fox, D. J. *Gaussian 09*, Revision B.01; Gaussian, Inc.: Wallingford, CT, 2010.
- (67) Becke, A. D. *J. Chem. Phys.* **1993**, *98*, 5648–5652.
- (68) Lee, C. T.; Yang, W. T.; Parr, R. G. *Phys. Rev. B* **1988**, *37*, 785–789.
- (69) Annibale, V. T.; Song, D. *RSC Adv.* **2013**, *3*, 11432–11449.
- (70) Gunanathan, C.; Milstein, D. *Acc. Chem. Res.* **2011**, *44*, 588–602.
- (71) Gunanathan, C.; Milstein, D. *Top. Organomet. Chem.* **2011**, *37*, 55–84.
- (72) Gunanathan, C.; Gnanaprakasam, B.; Iron, M. A.; Shimon, L. J. W.; Milstein, D. *J. Am. Chem. Soc.* **2010**, *132*, 14763–14765.
- (73) Grützmacher, H. *Angew. Chem., Int. Ed.* **2008**, *47*, 1814–1818.
- (74) Eckert, T. S.; Bruice, T. C. *J. Am. Chem. Soc.* **1983**, *105*, 4431–4441.
- (75) Riklin, M.; von Zelewsky, A.; Bashall, A.; McPartlin, M.; Baysal, A.; Connor, J.; Wallis, J. *Helv. Chim. Acta* **1999**, *82*, 1666–1680.
- (76) Siemeling, U.; Scheppelmann, I.; Neumann, B.; Stammler, H.; Schoeller, W. *Organometallics* **2004**, *23*, 626–628.
- (77) Phillips, A. D.; Zava, O.; Scopelliti, R.; Nazarov, A. A.; Dyson, P. J. *Organometallics* **2010**, *29*, 417–427.
- (78) Phillips, A. D.; Thommes, K.; Scopelliti, R.; Gandolfi, C.; Albrecht, M.; Severin, K.; Schreiber, D. F.; Dyson, P. J. *Organometallics* **2011**, *30*, 6119–6132.
- (79) Moreno, A.; Pregosin, P. S.; Laurenczy, G.; Phillips, A. D.; Dyson, P. J. *Organometallics* **2009**, *28*, 6432–6441.
- (80) Field, L.; Hambley, T.; Humphrey, P.; Masters, A.; Turner, P. *Inorg. Chem.* **2002**, *41*, 4618–4620.